5884 *Inorg. Chem.* **2009**, *48*, 5884–5890
DOI: 10.1021/ic900180x

Inorganic Chemistry
Article

Copper-, Cobalt-, and Manganese-Containing 17-Tungsto-2-Germanates

Nadeen H. Nsouli,[†] Amal H. Ismail,[†] Inga S. Helgadottir,[†] Michael H. Dickman,[†] Juan M. Clemente-Juan,[‡] and Ulrich Kortz*[,†]

[†]*School of Engineering and Science, Jacobs University, P.O. Box 750 561, 28725 Bremen, Germany, and* [‡]*Instituto de Ciencia Molecular, Fundació General de la Universidad de Valencia and Universidad de Valencia, Poligono La Coma s/n, 46980 Paterna, Spain*

Received January 28, 2009

The sandwich-type tungstogermanates $[Cu_3(H_2O)(B\text{-}\beta\text{-}GeW_9O_{33}(OH))(B\text{-}\beta\text{-}GeW_8O_{30}(OH))]^{12-}$ (**1**), $[Co(H_2O)_2\{Co_3(B\text{-}\beta\text{-}GeW_9O_{33}(OH))(B\text{-}\beta\text{-}GeW_8O_{30}(OH))\}_2]^{22-}$ (**2**), and $[Mn(H_2O)_2\{Mn_3(H_2O)(B\text{-}\beta\text{-}GeW_9O_{33}(OH))(B\text{-}\beta\text{-}GeW_8O_{30}(OH))\}_2]^{22-}$ (**3**) were synthesized and characterized by single-crystal X-ray diffraction, elemental analysis, thermogravimetric analysis, and infrared spectroscopy. Polyanion **1** is composed of two nonequivalent Keggin units, ($B\text{-}\beta\text{-}GeW_8O_{31}$) and ($B\text{-}\beta\text{-}GeW_9O_{34}$), linked to each other via three copper(II) ions in such a way that there is a plane of symmetry passing through both Ge atoms and the unique Cu atom, resulting in a sandwich-type structure with C_s symmetry. On the other hand, the monomeric building blocks of **2** and **3** contain the same Keggin fragments as **1**, but linked through three octahedrally coordinated Co^{2+} or Mn^{2+} ions. The major difference between complex **1** and complexes **2** and **3** is that the latter all lack a plane of symmetry due to a different orientation of the rotated triad. Magnetic measurements indicated antiferromagnetic exchange interactions between the three Cu^{2+} ions in **1** and between the three Mn^{2+} ions in **3**. On the other hand, polyanion **2** possesses ferromagnetic interaction of the Co^{2+} ions. The best least-squares fit values for **2** are $J_z = 7.9\ cm^{-1}$, $J_z = 3.1\ cm^{-1}$, $J_y = 2.4\ cm^{-1}$, $g_z = 6.77\ cm^{-1}$, and $g_{xy} = 4.15$ ($R = 2.6 \times 10^{-2}$).

Introduction

Polyoxometalates (POMs) are metal-oxide clusters formed of early d-block elements in high oxidation states (e.g., W^{6+}, V^{5+}), and they constitute a unique class of inorganic compounds. POMs were discovered in 1826 by Berzelius when he noted the formation of a yellow precipitate after the reaction of ammonium molybdate with phosphoric acid.[1] The chemistry of POMs is a rapidly growing field because they exhibit a combination of tunable properties, including composition, size, shape, charge density, redox potentials, and solubility.[2] As a result, POMs have potential applications in many fields such as catalysis, medicine, photochemistry, electrochemistry, and magnetism.[3] The mechanism of formation of polyanions is not well understood and is usually described as self-assembly. One important goal in POM synthesis is the incorporation of transition metals, lanthanides, organometallic entities, or any other functional unit(s) into lacunary (i.e., vacant) polyanion precursors, leading to a tremendous diversity of structures. In particular, polytungstates are of importance in this respect, as a large number of stable lacunary precursors are known (as opposed to polymolybdates or polyvanadates).

From a magnetic point of view, POMs containing more than one paramagnetic transition metal ion in close proximity may exhibit exchange-coupled spins. Polyanions with high-spin ground states and magnetic anisotropy are of technical interest in areas such as data storage and magnetic switches and so on.[4] In the past decades, much attention has

*To whom correspondence should be addressed. Fax: +49-(0)421-200-3229. E-mail: u.kortz@jacobs-university.de.

(1) Berzelius, J. J. *Pogg. Ann.* **1826**, *6*, 369.

(2) (a) Pope, M. T. *Heteropoly and Isopoly Oxometalates*; Springer: Berlin, 1983.(b) Pope, M. T.; Müller, A. Angew. Chem., Int. Ed. Engl. 1991, 30, 34. (c) Pope, M. T. In Comprehensive Coordination Chemistry II; McCleverty, J. A., Meyer, T. J., Eds.; Elsevier Ltd.: Oxford, U.K., 2004.(d) Hill, C. L. In Comprehensive Coordination Chemistry II; Wedd, A. G., Ed.; Elsevier Ltd.: Oxford, U.K., 2004.

(3) (a) *Polyoxometalates: From Platonic Solids to Anti Retroviral Activity*; Pope, M. T., Müller, A., Eds.; Kluwer: Dordrecht, The Netherlands, 1994.(b) Chem. Rev. 1998, 98, 1−389 (special thematic issue on polyoxometalates).(c) Polyoxometalate Chemistry: From Topology Via Self-Assembly to Applications; Pope, M. T., Müller A., Eds.; Kluwer: Dordrecht, The Netherlands, 2001.(d) Polyoxometalate Chemistry for Nano-Composite Design; Yamase, T., Pope, M. T., Eds.; Kluwer: Dordrecht, The Netherlands, 2002.(e) Polyoxometalate Molecular Science; Borrás-Almenar, J. J., Coronado, E., Müller, A., Pope, M. T., Eds.; Kluwer: Dordrecht, The Netherlands, 2003.(f) Vazylyev, M.; Sloboda-Rozner, D.; Haimov, A.; Maayan, G.; Neumann, R. Top. Catal. 2005, 34, 93.

(4) (a) Sessoli, R.; Gatteschi, D.; Caneschi, A.; Novak, M. A. *Nature* **1993**, *365*, 141. (b) Gambardella, P.; Rusponi, S.; Veronese, M.; Dhesi, S. S.; Grazioli, C.; Dallmeyer, A.; Cabria, I.; Zeller, R.; Dederichs, P. H.; Kern, K.; Carbone, C.; Brune, H. *Science* **2003**, *300*, 1130. (c) Long, J. R. In *Chemistry of Nanostructured Materials*; Yang, P., Ed.; World Scientific Publishing: Hong Kong, 2003; pp 241−315.(d) Bode, M.; Pietzsch, O.; Kubetzka, A.; Wiesendanger, R. *Phys. Rev. Lett.* **2004**, *92*, 067201. (e) Gatteschi, D.; Sessoli, R.; Villain, J. *Molecular Nanomagnets*; Oxford University Press: Oxford, U.K., 2006.

 Published on Web 06/01/2009

been devoted to the synthesis of transition-metal substituted POMs with multiple, spin-coupled magnetic centers in the area known as molecular magnetism.[5]

Transition-metal-containing POMs are usually prepared in a one-pot reaction of transition metal ions (e.g., Cu^{2+}, Fe^{3+}) with lacunary polytungstate precursors. In particular, the class of copper-containing POMs is very rich with respect to the number of Cu^{2+} ions and the shape of the magnetic cluster, for example, $[Cu_3(H_2O)_3(\alpha\text{-}XW_9O_{33})_2]^{n-}$ (n = 12, X = As^{III}, Sb^{III}; n = 10, X = Se^{IV}, Te^{IV}),[6] $[Cu_4(H_2O)_2(B\text{-}\alpha\text{-}XW_9O_{34})_2]^{n-}$ (X = P^V, As^V, n = 10; X = Si^{IV}, n = 12),[7] $[Cu_4K_2(H_2O)_8(\alpha\text{-}AsW_9O_{33})_2]^{8-}$,[8] $[Cu_5(OH)_4(H_2O)_2(A\text{-}\alpha\text{-}SiW_9O_{33})_2]^{10-}$,[9] $[\{(SiW_9O_{34})(SiW_9O_{33}(OH))(Cu(OH))_6Cu\}_2X]^{23-}$ (X = Cl, Br),[10] and $[Cu_{20}Cl(OH)_{24}(H_2O)_{12}(P_8W_{48}O_{184})]^{25-}$.[11]

However, the number of transition-metal-containing tungstogermanates is still limited. The subclass of organic–inorganic hybrid tungstogermanates includes a handful of structures. The group of Yang prepared $[Ni_4(Hdap)_2(B\text{-}\alpha\text{-}HGeW_9O_{34})_2]^{8-}$ (dap = 1,2-diaminopropane),[12] $[Cu_5(2,2'\text{-}bpy)_6\text{-}(H_2O)][B\text{-}\beta\text{-}GeW_8O_{31}]$, and $\{[Cu_5(2,2'\text{-}bpy)_5(H_2O)][B\text{-}\alpha\text{-}GeW_9O_{34}]\}_2$ (2,2′-bpy = 2,2′-bipyridine).[13] On the other hand, Niu et al. reported the copper-containing species $[Cu(DMF)_4(\alpha\text{-}GeW_{12}O_{40})_2]^{6-}$ (DMF = N,N-dimethylformamide),[14] $\{[Cu(phen)(\mu_2\text{-}CH_3COO)_2Cu(phen)(H_2O)]_2[Ge_2W_{23}CuO_{80}]\}^{8-}$ (phen = phenanthroline),[15] and $[Cu(en)_2(H_2O)]_2\{[Cu_4(GeW_9O_{34})_2][Cu(en)_2]\}^{3-}$.[16]

Our group has contributed several tungstogermanates with different incorporated or grafted transition metals: $[(RuC_6H_6)_2GeW_9O_{34}]^{6-}$,[17] $[Ru(dmso)_3(H_2O)GeW_{11}O_{39}]^{6-}$,[18] $[\{Ru(C_6H_6)(H_2O)\}\{Ru(C_6H_6)\}(\gamma\text{-}GeW_{10}O_{36})]^{4-}$,[19] $[Fe_6(OH)_3(A\text{-}\alpha\text{-}GeW_9O_{34}(OH)_3)_2]^{11-}$,[20] $K(H_2O)(\beta\text{-}Fe_2GeW_{10}O_{37}(OH))(\gamma\text{-}GeW_{10}O_{36})]^{12-}$ and $[\{\beta\text{-}Fe_2GeW_{10}O_{37}(OH)_2\}_2]^{12-}$,[21] and the Weakley-type dimers $[M_4(H_2O)_2(B\text{-}\alpha\text{-}GeW_9O_{34})_2]^{12-}$ (M = Mn^{2+}, Cu^{2+}, Zn^{2+}, Cd^{2+}).[22]

Other transition-metal-containing tungstogermanates include $[Cu_{10}(H_2O)_2(N_3)_4(GeW_9O_{34})_2(GeW_8O_{31})_2]^{24-}$,[23] $[Y(GeW_{11}O_{39})(H_2O)_2]^{5-}$,[24] $[Ti_6(OH)_3(GeW_9O_{37})_2]^{11-}$,[25] and the open Wells–Dawson structure $[\{Co(H_2O)\}(\mu\text{-}H_2O)_2K(Ge_2W_{18}O_{66})]^{13-}$.[26] Recently, Wang's group reported $[Mn_2(H_2O)_8Mn_4(H_2O)_2(B\text{-}\alpha\text{-}GeW_9O_{34})_2]^{8-}$, which is composed of Weakley-type $[Mn_4(H_2O)_2(B\text{-}\alpha\text{-}GeW_9O_{34})_2]^{12-}$ units connected via two Mn^{2+} ions forming a 1D chain.[27a] Yamase et al. reported the synthesis of $[Cu_4(GeW_9O_{34})_2]^{12-}$, showing a Cu_4^{8+} tetragon α-conjugated to two $[B\text{-}\alpha\text{-}GeW_9O_{34}]^{10-}$ Keggin moieties.[27b]

A few years ago, we reported the synthesis and structural characterization of the dilacunary decatungstogermanate $[\gamma\text{-}GeW_{10}O_{36}]^{8-}$.[28] Since then, we have been exploring its reactivity with various transition metal and rare earths ions, organometallic groups, and other electrophiles. Some of these results have already been published.[19,21] Here, we report on the synthesis and structural characterization of dimeric copper-, cobalt-, and manganese-containing tungstogermanates.

Experimental Section

Synthesis. All reagents were used as purchased without further purification. The dilacunary precursor $K_8[\gamma\text{-}GeW_{10}O_{36}]$ was synthesized according to the published procedure, and its purity was confirmed by infrared spectroscopy.[28]

$K_{12}[Cu_3(H_2O)(B\text{-}\beta\text{-}GeW_9O_{33}(OH))(B\text{-}\beta\text{-}GeW_8O_{30}(OH))]\cdot 31H_2O$ (K-1). A 0.05 g (0.28 mmol) sample of $CuCl_2\cdot 2H_2O$ was dissolved in 20 mL of a 1 M potassium acetate buffer at a pH of 4.8, followed by the addition of 0.50 g (0.17 mmol) of $K_8[\gamma\text{-}GeW_{10}O_{36}]\cdot 6H_2O$. Then, the solution was stirred and heated to 50 °C for 30 min. The solution was allowed to cool to room temperature and then was filtered. Slow evaporation of the solvent at room temperature for about one day led to the formation of light-green crystals suitable for X-ray diffraction. These crystals were isolated and air-dried (yield 0.08 g, 14%). IR for **K-1**: 940 (m), 900 (m), 872 (m), 815 (sh), 790 (sh), 766 (s), 713 (s), 503 (w), 449 (w), 430 (sh) cm^{-1}. Anal. calcd (%) for **K-1**: K, 8.5; W, 56.3; Cu, 3.4; Ge, 2.6. Found (%): K, 8.7; W, 55.2; Cu, 3.5; Ge, 2.7.

$K_{22}[Co(H_2O)_2\{Co_3(B\text{-}\beta\text{-}GeW_9O_{33}(OH))(B\text{-}\beta\text{-}GeW_8O_{30}(OH))\}_2]\cdot 52H_2O$ (K-2). The synthetic procedure was identical to that for **K-1**, but 0.07 g of $CoCl_2\cdot 6H_2O$ (0.28 mmol) was used instead of $CuCl_2\cdot 2H_2O$. Slow evaporation of the solvent at room temperature for two weeks resulted in dark-purple crystals. These crystals were isolated and air-dried (yield 0.07 g, 13%). IR for **K-2**: 941 (m), 889 (m), 867 (m), 841 (m),

(5) (a) Yamase, T.; Botar, B.; Ishikawa, E.; Fukaya, K. *Chem. Lett.* **2001**, 56. (b) Laronze, N.; Marrot, J.; Hervé, G. *Inorg. Chem.* **2003**, *42*, 5857. (c) Anderson, T. M.; Neiwert, W. A.; Hardcastle, K. I.; Hill, C. L. *Inorg. Chem.* **2004**, *43*, 7353. (d) Nellutla, S.; van Tol, J.; Dalal, N. S.; Bi, L. H.; Kortz, U.; Keita, B.; Nadjo, L.; Khitrov, G. A.; Marshall, A. G. *Inorg. Chem.* **2005**, *44*, 9795. (e) Godin, B.; Chen, Y. G.; Vaissermann, J.; Ruhlmann, L.; Verdaguer, M.; Gouzerh, P. *Angew. Chem., Int. Ed.* **2005**, *44*, 3072. (f) Godin, B.; Vaissermann, J.; Herson, P.; Ruhlmann, L.; Verdaguer, M.; Gouzerh, P. *Chem. Commun.* **2005**, 5624. (g) Pichon, C.; Mialane, P.; Dolbecq, A.; Marrot, J.; Rivière, E.; Keita, B.; Nadjo, L.; Sécheresse, F. *Inorg. Chem.* **2007**, *46*, 5292. (h) Kortz, U.; Müller, A.; van Slageren, J.; Schnack, J.; Dalal, N. S.; Dressel, M. *Coord. Chem. Rev.* **2009**, 253, in press.

(6) Kortz, U.; Al-Kassem, N. K.; Savelieff, M. G.; Al Kadi, N. A.; Sadakane, M. *Inorg. Chem.* **2001**, *40*, 4742.

(7) (a) Weakley, T. J. R.; Finke, R. G. *Inorg. Chem.* **1990**, *29*, 1235. (b) Kortz, U.; Isber, S.; Dickman, M. H.; Ravot, D. *Inorg. Chem.* **2000**, *39*, 2915. (c) Bi, L.-H.; Huang, R.-D.; Peng, J.; Wang, E.-B.; Wang, Y. H.; Hu, C.-W. *J. Chem. Soc., Dalton Trans.* **2001**, 121.

(8) Kortz, U.; Nellutla, S.; Stowe, A. C.; Dalal, N. S.; van Tol, J.; Bassil, B. S. *Inorg. Chem.* **2004**, *43*, 144.

(9) Bi, L.-H.; Kortz, U. *Inorg. Chem.* **2004**, 7961.

(10) Mialane, P.; Dolbecq, A.; Marrot, J.; Rivière, E.; Sécheresse, F. *Angew. Chem., Int. Ed.* **2003**, *42*, 3523.

(11) Mal, S. S.; Kortz, U. *Angew. Chem., Int. Ed.* **2005**, *44*, 3777.

(12) Zhao, J.-W.; Li, B.; Zheng, S.-T.; Yang, G.-Y. *Cryst. Growth Des.* **2007**, *7*, 2658.

(13) Wang, C.-M.; Zheng, S.-T.; Yang, G.-Y. *Inorg. Chem.* **2007**, *46*, 616.

(14) Niu, J.-Y.; Han, Q.-X.; Wang, J.-P. *J. Coord. Chem.* **2003**, *56*, 523.

(15) Wang, J.-P.; Ren, Q.; Zhao, J.-W.; Niu, J.-Y. *Inorg. Chem. Commun.* **2006**, *9*, 1281.

(16) Wang, J.-P.; Du, X.-D.; Niu, J.-Y. *Chem. Lett.* **2006**, *35*, 1408.

(17) Bi, L.-H.; Kortz, U.; Dickman, M. H.; Keita, B.; Nadjo, L. *Inorg. Chem.* **2005**, *44*, 7485.

(18) Bi, L.-H.; Kortz, U.; Keita, B.; Nadjo, L. *Dalton Trans.* **2004**, 3184.

(19) Bi, L.-H.; Chubarova, E. V.; Nsouli, N. H.; Dickman, M. H.; Kortz, U.; Keita, B.; Nadjo, L. *Inorg. Chem.* **2006**, *45*, 8575.

(20) Bi, L.-H.; Kortz, U.; Nellutla, S.; Stowe, A. C.; Dalal, N. S.; Keita, B.; Nadjo, L. *Inorg. Chem.* **2005**, *44*, 896.

(21) Nsouli, N. H.; Mal, S. S.; Dickman, M. H.; Kortz, U.; Keita, B.; Nadjo, L.; Clemente-Juan, J. M. *Inorg. Chem.* **2007**, *46*, 8763.

(22) Kortz, U.; Nellutla, S.; Stowe, A. C.; Dalal, N. S.; Rauwald, U.; Danquah, W.; Ravot, D. *Inorg. Chem.* **2004**, *43*, 2308.

(23) Zhang, Z.; Qi, Y.; Qin, C.; Li, Y.; Wang, E.; Wang, X.; Su, Z.; Xu, L. *Inorg. Chem.* **2007**, *46*, 8162.

(24) Wang, J.-P.; Duan, X.-Y.; Du, X.-D.; Niu, J.-Y. *Cryst. Growth Des.* **2006**, *6*, 2266.

(25) Yamase, T.; Ozeki, T.; Sakamoto, H.; Nishiya, S.; Yamamoto, A. *Bull. Chem. Soc. Jpn.* **1993**, *66*, 103.

(26) Sun, C.-Y.; Liu, S.-X.; Wang, C.-L.; Xie, L.-H.; Zhang, C.-D.; Bo, G.; Su, Z.-M.; Jia, H.-Q. *J. Mol. Struct.* **2006**, *785*, 170.

(27) (a) Gan, X.; Zhang, Z.; Yao, S.; Chen, W.; Wang, E.; Zhang, H. *J. Clust. Sci.* **2008**, *19*, 401. (b) Yamase, T.; Abe, H.; Ishikawa, E.; Nojiri, H.; Ohshima, Y. *Inorg. Chem.* **2009**, *48*, 138.

(28) Nsouli, N. H.; Bassil, B. S.; Dickman, M. H.; Kortz, U.; Keita, B.; Nadjo, L. *Inorg. Chem.* **2006**, *45*, 3858.

Table 1. Crystal Data and Structure for **K-1**, **K-2**, and **K-3**

	K-1	K-2	K-3
empirical formula	$H_{66}Cu_3Ge_2K_{12}O_{97}W_{17}$	$H_{112}Co_7Ge_4K_{22}O_{184}W_{34}$	$H_{102}Ge_4K_{22}Mn_7O_{179}W_{34}$
fw	5549.0	10870.9	10752.9
T (K)	173(2)	173(2)	296(2)
wavelength (Å^3)	0.71073	0.71073	0.71073
crystal system	triclinic	monoclinic	triclinic
space group	$P\bar{1}$	$P2_1/n$	$P\bar{1}$
a (Å)	12.6684(3)	19.593(7)	12.2372(16)
b (Å)	20.7927(5)	24.700(13)	17.9117(18)
c (Å)	33.4049(8)	34.010(13)	18.963(3)
α (deg)	83.4747(12)	90	91.154(4)
β (deg)	80.1672(14)	101.626(13)	96.737(5)
γ (deg)	73.8061(12)	90	101.122(4)
V (Å^3)	8305.7(3)	16121(12)	4046.4(9)
Z	4	4	1
d_{calcd} (Mg/m^3)	4.438	4.479	4.413
abs coeff (mm^{-1})	25.64	26.28	26.00
goodness-of-fit on F^2	1.01	1.07	1.07
$R\,[I > 2\sigma(I)]^a$	0.050	0.070	0.079
R_w (all data)^b	0.148	0.205	0.230

$^a R = \sum ||F_o| - |F_c|| / \sum |F_o|$. $^b R_w = [\sum w(F_o^2 - F_c^2)^2 / \sum w(F_o^2)^2]^{1/2}$.

812 (sh), 789 (s), 764 (s), 696 (s), 506 (w), 449 (m) cm^{-1}. Anal. calcd (%) for **K-2**: K, 7.9; W, 57.5; Co, 3.8; Ge, 2.7. Found (%): K, 7.0; W, 56.9; Co, 3.5; Ge, 2.5.

$K_{22}[Mn(H_2O)_2\{Mn_3(H_2O)(B\text{-}\beta\text{-}GeW_9O_{33}(OH))(B\text{-}\beta\text{-}GeW_8O_{30}(OH))\}_2]\cdot 45H_2O$ (K-3). The synthetic procedure was identical to that for **K-1**, but 0.06 g of $MnCl_2\cdot 4H_2O$ (0.28 mmol) was used instead of $CuCl_2\cdot 2H_2O$. Slow evaporation of the solvent at room temperature for one day resulted in yellow crystals. These crystals were isolated and air-dried (yield 0.08 g, 15%). IR for **K-3**: 940 (m), 870 (m), 852 (m), 805 (sh), 789 (s), 764 (s), 706 (m), 520 (w), 494 (w), 449 (m) cm^{-1}. Anal. calcd for **K-3**: K, 8.0; W, 58.1; Mn, 3.6; Ge, 2.7. Found (%): K, 7.1; W, 57.3; Mn, 3.8; Ge, 2.4.

Instrumentation. Infrared spectra were recorded on a Nicolet Avatar 370 FT-IR spectrophotometer using KBr pellets. The following abbreviations were used to assign the peak intensities: w = weak, m = medium, s = strong, and sh = shoulder. Elemental analyses for **K-1**, **K-2**, and **K-3** were performed by ANALYTIS, Wesseling, Germany. Thermogravimetric analyses were carried out on a TA Instruments SDT Q600 thermobalance with a 100 mL/min flow of nitrogen; the temperature was ramped from 20 to 800 °C at a rate of 2 °C/min.

X-Ray Crystallography. Crystals were mounted on a Hampton cryoloop in light oil for data collection at −100 °C. Indexing and data collection were performed on a Bruker D8 SMART APEX II CCD diffractometer with κ geometry and Mo Kα radiation (graphite monochromator, λ = 0.71073 Å). Data integration was performed using *SAINT*.[29] Routine Lorentz and polarization corrections were applied. Multiscan absorption corrections were performed using *SADABS*.[30] Direct methods (*SHELXS97*) successfully located the tungsten atoms, and successive Fourier syntheses (*SHELXL97*) revealed the remaining atoms.[30] Refinements were full-matrix least-squares against F^2 using all data. In the final refinement, all nondisordered heavy atoms were refined anisotropically; oxygen atoms and disordered cations were refined isotropically. No hydrogen atoms were included in the models. Crystallographic data are summarized in Table 1.

Results and Discussion

Synthesis and Structure. Reaction of $CuCl_2\cdot 2H_2O$, $CoCl_2\cdot 6H_2O$, or $MnCl_2\cdot 4H_2O$ with $K_8[\gamma\text{-}GeW_{10}O_{36}]\cdot 6H_2O$ in a ratio of 1.5:1 in a potassium acetate buffer (pH 4.8) at 50 °C resulted in the sandwich-type tungstogermanates $[Cu_3(H_2O)(B\text{-}\beta\text{-}GeW_9O_{33}(OH))(B\text{-}\beta\text{-}GeW_8O_{30}(OH))]^{12-}$ (**1**), $[Co(H_2O)_2\{Co_3(B\text{-}\beta\text{-}GeW_9O_{33}(OH))(B\text{-}\beta\text{-}GeW_8O_{30}(OH))\}_2]^{22-}$ (**2**), and $[Mn(H_2O)_2\{Mn_3(H_2O)(B\text{-}\beta\text{-}GeW_9O_{33}(OH))(B\text{-}\beta\text{-}GeW_8O_{30}(OH))\}_2]^{22-}$ (**3**), respectively.

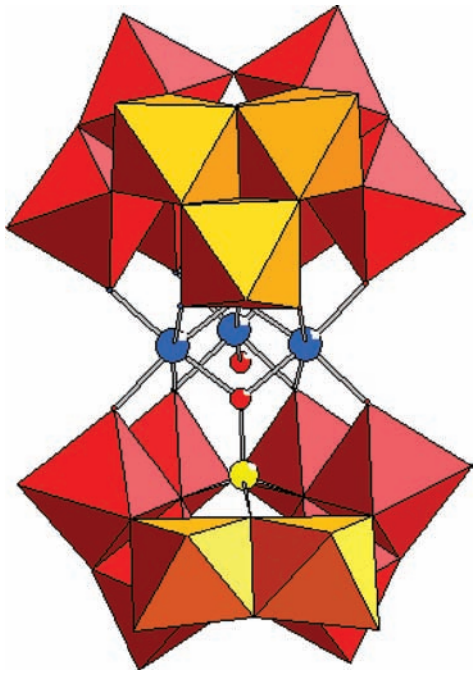

Figure 1. Combined ball-and-stick/polyhedral representation of $[Cu_3(H_2O)(B\text{-}\beta\text{-}GeW_9O_{33}(OH))(B\text{-}\beta\text{-}GeW_8O_{30}(OH))]^{12-}$ (**1**). Polyhedra represent WO_6 (red or orange) and the balls represent germanium (yellow), copper (blue) and oxygen (red). The rotated WO_6 octahedra are shown in orange for clarity.

Polyanion **1** is composed of two nonequivalent Keggin units, ($B\text{-}\beta\text{-}GeW_8O_{31}$) and ($B\text{-}\beta\text{-}GeW_9O_{34}$). These two units are held together by three copper(II) ions in such a way that there is a plane of symmetry passing through both Ge atoms and the unique Cu atom, resulting in a sandwich-type structure with C_s symmetry (Figure 1).

(29) *SAINT*; Bruker AXS Inc.: Madison, WI, 2007.
(30) Sheldrick, G. M. *Acta Crystallogr.* **2007**, *A64*, 112.

Scheme 1. Possible Two-Step Transformation Pathway of $[\gamma\text{-}GeW_{10}O_{36}]^{8-}$ Resulting First in (B-β-GeW_8O_{31}) via a Loss of Two Edge-Shared, Rotated WO_6 Octahedra and Then in (B-β-GeW_9O_{34}) via Gain of a WO_6 Unit Forming a Complete Rotated Triad[a]

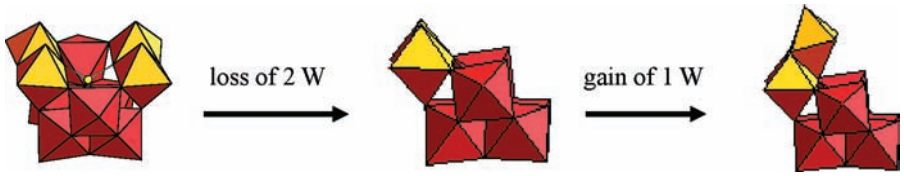

[a] The color code is the same as in Figure 1.

Each Keggin fragment in **1** is linked to three Jahn−Teller distorted octahedral Cu^{2+} ions. The Cu atoms are linked to each of the lacunary units via two Cu−O−W bonds. The two structurally equivalent Cu atoms are also linked to an oxygen atom of each GeO_4 hetero group. The unique Cu completes its octahedral coordination sphere by an oxygen atom of the GeO_4 hetero group of the (B-β-GeW_9O_{34}) fragment and a terminal water ligand.

We also performed bond valence sum (BVS) calculations for **1**, and the values for O2C (1.26), O117 (1.12), and O1Cu (0.09) indicate monoprotonation of the first two and diprotonation of the latter.[31] The presence of two hydroxo and one aqua ligand in **1** results in a total polyanion charge of −12.

We believe that both tungstogermanate fragments in **1** are formed by the decomposition of $[\gamma\text{-}GeW_{10}O_{36}]^{8-}$. Scheme 1 indicates a possible two-step transformation pathway of $[\gamma\text{-}GeW_{10}O_{36}]^{8-}$, resulting first in ($B$-$\beta$-$GeW_8O_{31}$) via a loss of two edge-shared, rotated WO_6 octahedra and then in (B-β-GeW_9O_{34}) via a gain of a WO_6 unit, forming a complete, rotated triad. Such a transformation has a precedent in tungstosilicate chemistry, namely, for $[\gamma\text{-}SiW_{10}O_{36}]^{8-}$, which is the well-known silicon analogue of $[\gamma\text{-}GeW_{10}O_{36}]^{8-}$.[32] Our group observed both the (B-β-SiW_9O_{34}) and (B-β-SiW_8O_{31}) fragments in the three-cobalt(II)-containing $[Co_3(H_2O)(B\text{-}\beta\text{-}SiW_9O_{33}(OH))(B\text{-}\beta\text{-}SiW_8O_{29}(OH)_2)]^{11-}$,[32a] and only the ($B$-$\beta$-$SiW_8O_{31}$) fragment in the 15-Co(II)-containing $[Co_6(H_2O)_{30}\{Co_9Cl_2(OH)_3(H_2O)_9(B\text{-}\beta\text{-}SiW_8O_{31})_3\}]^{5-}$.[32c] The germanium analogue of the tetralacunary fragment (β-GeW_8O_{31}) was first observed by Wang et al. in the copper-containing $[Cu_5(2,2'\text{-bpy})_6(H_2O)][GeW_8O_{31}]\cdot 9H_2O$.[13]

Polyanion **1** is similar in structure to our cobalt(II)-containing tungstosilicate $[Co_3(H_2O)(B\text{-}\beta\text{-}SiW_9O_{33}(OH))(B\text{-}\beta\text{-}SiW_8O_{29}(OH)_2)]^{11-}$, which forms a dimer in the solid state.[32a] The Cu_3-containing **1** has C_s symmetry, with the plane of symmetry passing through the rotated W_3O_{13} triad of the (B-β-GeW_9O_{34}) fragment. This is not the case for the asymmetrical Co_3-containing tungstosilicate which possesses C_1 symmetry because the rotated W_3O_{13} triad is located "on the side". Cronin et al. have recently shown that $[Co_3(H_2O)(B\text{-}\beta\text{-}SiW_9O_{34})(B\text{-}\beta\text{-}SiW_8O_{29}(OH)_2)]^{12-}$ can be synthesized at a pH of 8.0, and when the pH was increased to 8.8, $[Co_3(H_2O)(B\text{-}\alpha\text{-}SiW_9O_{34})(B\text{-}\beta\text{-}SiW_8O_{31})]^{14-}$ was formed.[32e] The structure of the former is identical to our $[Co_3(H_2O)(B\text{-}\beta\text{-}SiW_9O_{33}(OH))(B\text{-}\beta\text{-}SiW_8O_{29}(OH)_2)]^{11-}$ (vide supra), but it did not dimerize in the solid state. On the other hand, the latter contains a (B-α-SiW_9O_{34}) Keggin unit rather than a (B-β-SiW_9O_{34}) fragment. Our $[Co_3(H_2O)(B\text{-}\beta\text{-}SiW_9O_{33}(OH))(B\text{-}\beta\text{-}SiW_8O_{29}(OH)_2)]^{11-}$, which represents the Si analogue of polyanion **2**, was formed as a mixed potassium/sodium salt in a 0.5 M sodium acetate buffer (pH 4.8) using a $CoCl_2\cdot 6H_2O$ to $K_8[\gamma\text{-}SiW_{10}O_{36}]\cdot 6H_2O$ ratio of 2:1.[32a] On the other hand, the sodium salt of the satellite-shaped Co-15 silicotungstate $[Co_6(H_2O)_{30}\{Co_9Cl_2(OH)_3(H_2O)_9(B\text{-}\beta\text{-}SiW_8O_{31})_3\}]^{5-}$ was prepared in a 13:1 ratio of the above reagents in a 1 M NaCl medium, and the pH was adjusted to 5.5 by the addition of 0.1 M NaOH.[32c]

It is also of interest to compare **1** to Wang and coworkers' copper-containing tungstogermanate $[Cu_{10}(H_2O)_2(N_3)_4(B\text{-}\alpha\text{-}GeW_9O_{34})_2(B\text{-}\beta\text{-}GeW_8O_{31})_2]^{24-}$.[23] The latter consists of a $\{Cu_{10}(N_3)_4\}$cluster, two (B-β-GeW_8O_{31}) units, and two (B-α-GeW_9O_{34}) units, forming two equivalent sandwich fragments. Each fragment is composed of a (B-β-GeW_8O_{31}) and a (B-α-GeW_9O_{34}) unit linked by four Cu^{2+} ions. One of the Cu^{2+} ions is linked to three nitrogens of three azide groups and to three oxygens of the neighboring Cu atoms. Two of the azide ligands form a linkage with the two equivalent sandwich fragments. The fifth Cu^{2+} ion is coordinated to four oxygen atoms and to two azide ligands, one of which holds the two fragments together.

The cobalt-containing polyanion $[Co(H_2O)_2\{Co_3(B\text{-}\beta\text{-}GeW_9O_{33}(OH))(B\text{-}\beta\text{-}GeW_8O_{30}(OH))\}_2]^{22-}$ (**2**) contains two equivalent sandwich-type fragments $[Co_3(B\text{-}\beta\text{-}GeW_9O_{33}(OH))(B\text{-}\beta\text{-}GeW_8O_{30}(OH))]^{12-}$ (**2a**) arranged almost orthogonally to each other and linked via two equivalent Co−O−W bonds. Each fragment **2a** comprises a (B-β-GeW_8O_{31}) and a (B-β-GeW_9O_{34}) capping a triangular cobalt(II) cluster. These structural aspects resemble our previously reported tungstosilicate $[Co_3(H_2O)(B\text{-}\beta\text{-}SiW_9O_{33}(OH))(B\text{-}\beta\text{-}SiW_8O_{29}(OH)_2)]^{11-}$.[32a] In **2**, the presence of an extra cobalt(II) ion (with two trans-aqua ligands) ensures the formation of a 1-D network via coordination to the pairs of rotated WO_6 groups within each (B-β-GeW_8O_{31}) unit (Figure 2).

Both polyanions **1** and **2a** are composed of the same Keggin fragments, but there is still a major difference between them. Polyanion **1** has a plane of symmetry which passes through the rotated triad of the (B-β-GeW_9O_{34}) unit (Figure 3a), while **2a** lacks a plane of

(31) Brown, I. D.; Altermatt, D. *Acta Crystallogr.* **1985**, *B41*, 244.

(32) (a) Bassil, B. S.; Kortz, U.; Tigan, A. S.; Clemente-Juan, J. M.; Keita, B.; de Oliveira, P.; Nadjo, L. *Inorg. Chem.* **2005**, *44*, 9360. (b) Mialane, P.; Dolbecq, A.; Marrot, J.; Rivière, E.; Sécheresse, F. *Chem.—Eur. J.* **2005**, *11*, 1771. (c) Bassil, B. S.; Nellutla, S.; Kortz, U.; Stowe, A. C.; van Tol, J.; Dalal, N. S.; Keita, B.; Nadjo, L. *Inorg. Chem.* **2005**, *44*, 2659. (d) Lisnard, L.; Mialane, P.; Dolbecq, A.; Marrot, J.; Clemente-Juan, J. M.; Coronado, E.; Keita, B.; Oliveira, P. D.; Nadjo, L.; Sécheresse, F. *Chem.—Eur. J.* **2007**, *13*, 3525. (e) Mitchell, S. G.; Ritchie, C.; Long, D. L.; Cronin, L. *Dalton Trans.* **2008**, 1415.

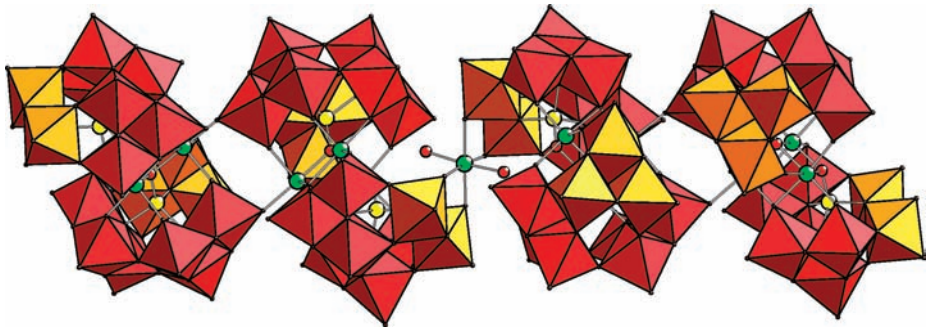

Figure 2. Combined ball-and-stick/polyhedral presentation of the solid-state arrangement of **2**. The polyhedra represent WO_6 (red or orange) and the balls represent germanium (yellow), cobalt (green) and oxygen (red).

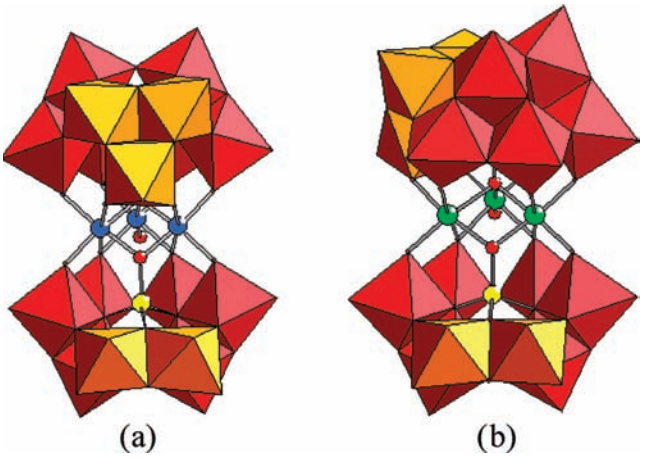

Figure 3. Polyhedral representation of the copper(II)-containing **1** (left, a) and the cobalt(II)-containing fragment **2a** (right, b). Notice the different orientation of the rotated triad in the respective "upper" (*B*-β-GeW_9O_{34}) units.

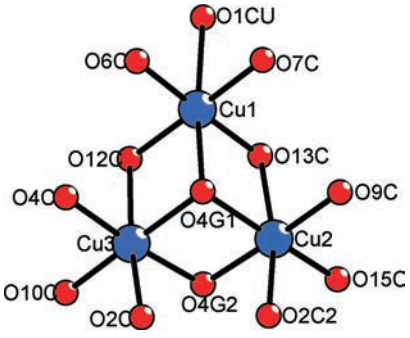

Figure 4. Ball-and-stick representation of the Cu_3 core of **1** and the labeling scheme.

symmetry due to the positioning of the rotated triad "on the side" of the polyanion (Figure 3b).

We believe that the different electron configurations and hence coordination geometries of Cu^{2+} (d^9) and Co^{2+} (high-spin d^7) are most likely the origin of the structural differences for **1** and **2a**. Copper(II) ions exhibit the well-known Jahn−Teller distortion, resulting in axially elongated octahedral coordination. It appears that such a distorted trinuclear copper(II) cluster (Figure 4) can be accommodated better in the cisoid conformation of **1**, whereas the trinuclear cobalt(II) cluster can be accommodated better in the transoid conformation of **2a**. Taking a closer look at the Cu−O bond lengths in **1** indicates that

Table 2. Selected Cu−O and Co−O Bond Lengths [Å] for **1** and **2**, Respectively[a]

1		**2**	
Cu(1)−O(6C)$_{eq}$	1.91(1)	Co(1)−O	1.97(3), 2.00(2),
Cu(1)−O(13C)$_{eq}$	1.94(1)		2.02(2), 2.03(3),
Cu(1)−O(7C)$_{eq}$	1.95(1)		2.04(2), 2.21(2)
Cu(1)−O(12C)$_{eq}$	1.99(1)	Co(2)−O	2.02(2), 2.06(2),
av. Cu(1)−O$_{eq}$	**1.95(1)**		2.06(2), 2.12(2),
			2.15(2), 2.25(2)
Cu(2)−O(15C)$_{eq}$	1.93(1)	Co(3)−O	2.06(2), 2.08(2),
Cu(2)−O(4G2)$_{eq}$	1.96(1)		2.08(3), 2.09(2),
Cu(2)−O(4G1)$_{eq}$	1.97(1)		2.09(2), 2.12(2)
Cu(2)−O(9C)$_{eq}$	1.98(1)	Co(4)−O	2.04(3), 2.07(2),
av. Cu(2)−O$_{eq}$	**1.96(1)**		2.08(2), 2.09(2),
			2.12(3), 2.18(2)
Cu(3)−O(4G2)$_{eq}$	1.97(1)	Co(5)−O	2.03(2), 2.03(2),
Cu(3)−O(4C)$_{eq}$	1.98(1)		2.04(3), 2.05(2),
Cu(3)−O(10C)$_{eq}$	1.98(1)		2.08(2), 2.19(2)
Cu(3)−O(4G1)$_{eq}$	2.00(1)	Co(6)−O	2.04(2), 2.05(2),
av. Cu(3)−O$_{eq}$	**1.98(1)**		2.06(2), 2.07(2),
			2.11(2), 2.17(2)
Cu(1)−O(4G1)$_{ax1}$	2.35(1)		
Cu(2)−O(2C2)$_{ax1}$	2.30(1)		
Cu(3)−O(2C)$_{ax1}$	2.31(1)		
av. Cu−O$_{ax1}$	**2.32(1)**		
Cu(1)−O(1CU)$_{ax2}$	2.55(2)		
Cu(2)−O(13C)$_{ax2}$	2.54(1)		
Cu(3)−O(12C)$_{ax2}$	2.52(1)		
av. Cu−O$_{ax2}$	**2.54(1)**		

[a] Mean values are indicated in bold.

the equatorial bonds are in the normal range (Cu1−O$_{eq}$ 1.95(3) Å, Cu2−O$_{eq}$ 1.96(2) Å, and Cu3−O$_{eq}$ 1.98(1) Å). As expected, the axial Cu−O bonds are longer and actually fall in the two categories, long and very long (Cu1−O$_{ax}$ 2.35(1), 2.55(1) Å; Cu2−O$_{ax}$ 2.30(1), 2.54(1) Å; and Cu3−O$_{ax}$ 2.31(1), 2.52(1) Å) (Table 2).

We also performed BVS calculations for **2**. The values for two of the oxygens, O2C7 (0.23) and O3C7 (0.29), connected to the Co linker in **2** show that they are diprotonated. In addition, we discovered monoprotonation in each of the (*B*-β-GeW_9O_{34}) units, one of them being O26A (1.10) in the first sandwich-type fragment and the second being O3C3 (1.09) in the other fragment. Moreover, a proton is disordered over two positions in each (*B*-β-GeW_8O_{31}) unit. The first proton is shared by oxygens O137 (1.27) and O146 (1.40) in the first fragment and the other by O272 (1.53) and O283 (1.43).

The manganese(II)-containing polyanion **3** is composed of two fragments of $[Mn_3(H_2O)(B\text{-}\beta\text{-}GeW_9O_{33}(OH))(B\text{-}\beta\text{-}GeW_8O_{30}(OH))]^{12-}$ linked through an octahedrally coordinated Mn^{2+} ion. In close analogy to **2**, this extra metal ion links the two sandwich fragments by coordinating

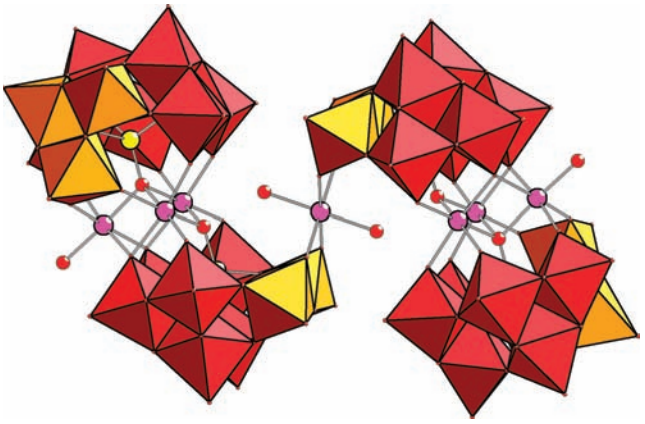

Figure 5. Combined polyhedral/ball-and-stick representation of **3**. The pink spheres represent Mn^{2+} (**3**). Otherwise, the color code is the same as in Figures 1−3.

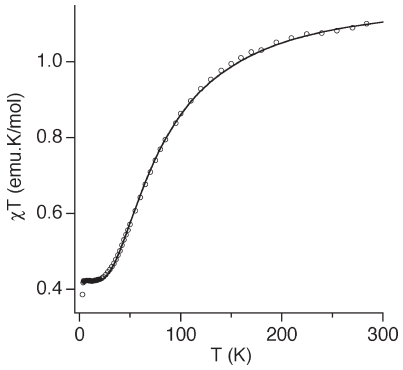

Figure 6. Plot of the product $\chi_m T$ as a function of T for **K-1**.

to the pair of rotated tungsten centers in each (B-β-GeW_8O_{31}) unit, and it also has two trans-related terminal water ligands (Figure 5). Polyanion **3** exhibits a small degree (∼15%) of crystallographic α/β disorder of two W_3O_{13} triads in the (B-β-GeW_9O_{34}) unit. We were able to resolve this issue by assigning partial occupancies to the involved W atoms.

Magnetic Susceptibility. The temperature dependence of the product $\chi_m T$ and low-temperature magnetizations of a powder sample of **K-1** were collected in the temperature range 2−300 K at 0.1 T and in the field range 0−5 T at 2 and 5 K, respectively. The product $\chi_m T$ (see Figure 6) shows a continuous decrease between 300 and 20 K from 1.1 to 0.42 emu K/mol. Below 20 K, a plateau is reached with a constant value around 0.42 emu K/mol. Only at very low temperatures, 3 K, does the $\chi_m T$ drop again due to a smaller contribution as anisotropy or a field effect. The magnetization curves (see Figure 7) increase almost linearly up to 3 K and then tend to approach saturation. The temperature dependence suggests antiferromagnetic interactions between the three Cu^{2+} ions ($S = 1/2$). In order to reproduce the magnetic behavior, we can propose the following isotropic exchange Hamiltonian: $H = -2J_1(\hat{S}_1\hat{S}_2 + \hat{S}_1\hat{S}_3) - 2J_2\hat{S}_2\hat{S}_3$. The best least-squares fit results in this set of parameters: $J_1 = -6.50\ cm^{-1}$, $J_2 = -47.0\ cm^{-1}$, and $g = 2.13$ ($R = 3.9 \times 10^{-5}$). These parameters also reproduce in good agreement both magnetization curves.

The parameters obtained are similar to other, related copper(II)-containing polytungstates. Due to the nature

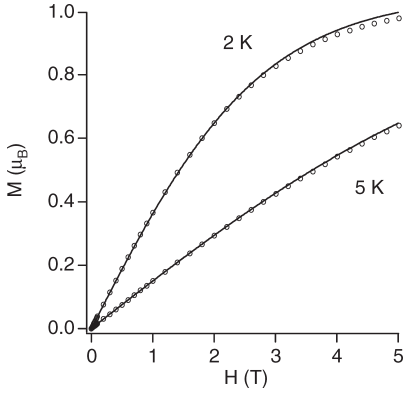

Figure 7. Magnetization data at 2 and 5 K for **K-1**.

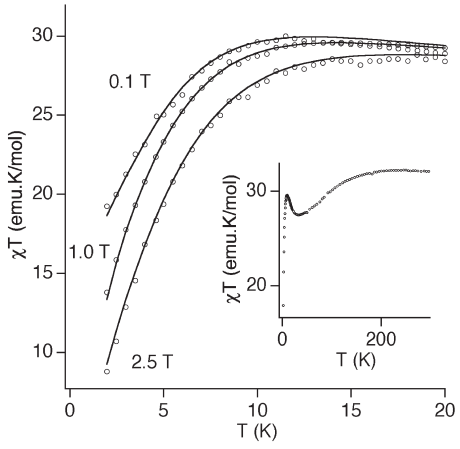

Figure 8. Plot of the product $\chi_m T$ vs T in the range 2−20 K at different fields (0.1, 1.0, and 2.0 T) for **K-2**. Inset: Plot of the product $\chi_m T$ vs T in the range 2−300 K at 0.1 for **K-2**.

of the encapsulating fragments, the most closely related cluster is the Cu_4O_{16} tetramer.[22] In this case, the values of the exchange parameters are $J_1 = -11\ cm^{-1}$ and $J_2 = -82\ cm^{-1}$. We can see that these values are around double those for **K-1**, but the ratio J_2/J_1 is the same in both cases, 7.2−7.5. The situation is similar for other related Cu_4O_{16} tetramers where this ratio is around 4.[7a,33] This can be attributed to different types of Cu···Cu interactions. J_2 is associated with short Cu−O bridges and J_1 with long ones. The Cu_3O_3 fragment in **1** can be considered a pseudocubane with one short and two long distances, 1 + 2 (see Figure 4). Recently, a magnetostructural correlation study[34] on Cu_4O_4 core cubanes demonstrated that, in systems with two short and four long distances, 2 + 4 (if we remove one Cu to transform into our Cu_3O_3 1 + 2 core), the leading strong antiferromagnetic interaction corresponds to the short distance pathway and the other long one can be weakly antiferromagnetic or weakly ferromagnetic.

The $\chi_m T$ product versus T for polyanion salt **K-2** shows a continuous decrease from room temperature (32.1 emu K/mol) to a minimum at 32 K (Figure 8). This behavior can be associated with the spin−orbit coupling of the Co^{2+} ions. Below this temperature, a maximum is observed at

(33) Gómez-García, C. J.; Coronado, E.; Borrás-Almenar, J. J. *Inorg. Chem.* **1992**, *31*, 1667.
(34) Tercero, J.; Ruiz, E.; Alvarez, S.; Rodríguez-Fortea, A.; Alemany, P. *J. Mater. Chem.* **2006**, *16*, 2729.

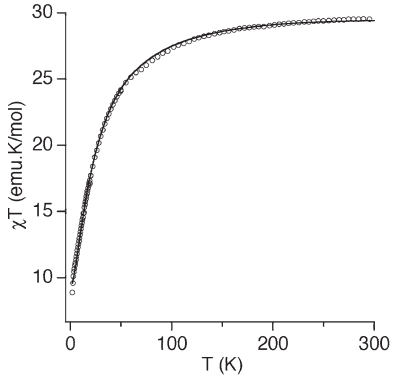

Figure 9. Plot of the product $\chi_m T$ as a function of T for **K-3**.

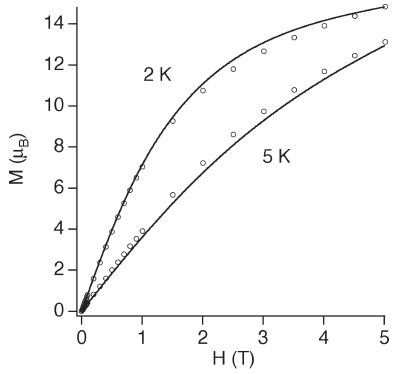

Figure 10. Magnetization data at 2 and 5 K for **K-3**.

11 K (29.9 emu K/mol). This maximum indicates the ferromagnetic interaction between the lowest Kramers doublets with an effective spin of 1/2. The anisotropic exchange Hamiltonian used to fit polyanion **2** can be written as two identical trinuclear contibutions, $\hat{H} = -2\sum_{\alpha=x,y,x} J_\alpha(\hat{S}_1{}^\alpha\hat{S}_2{}^\alpha + \hat{S}_1{}^\alpha\hat{S}_3{}^\alpha + \hat{S}_2{}^\alpha\hat{S}_3{}^\alpha)$, and the contribution of an isolated Co^{2+} ion. Taking into account this exchange Hamiltonian and a simultaneous fit of the three magnetic susceptibilities at different fields, the best least-squares fit values are $J_z = 7.9\ cm^{-1}$, $J_z = 3.1\ cm^{-1}$, $J_y = 2.4\ cm^{-1}$, $g_z = 6.77\ cm^{-1}$, and $g_{xy} = 4.15$ ($R = 2.6 \times 10^{-2}$). It is well-known that the ferromagnetic interaction is due to the orthogonality of the magnetic orbitals in edge-shared CoO_6 octahedra. Compared with other, similar compounds, we see that the values obtained are of the same order of magnitude as those reported in the literature.[32a,32b,35]

The magnetic properties of the polyanion salt **K-3** in the form of a $\chi_m T$ versus T plot and low-temperature magnetization are shown in Figures 9 and 10, respectively. At room temperature, $\chi_m T$ is equal to 29.6 emu K/mol, a value close to seven isolated manganese(II) ions ($S = 5/2$). As the temperature is lowered, the $\chi_m T$ product decreases to reach a value of 8.9 emu K/mol at 2 K. This temperature dependence can be associated with antiferromagnetic interaction between the three Mn^{2+} ions of each trinuclear fragment. In order to fit the magnetic data for **K-3**, we can use the same isotropic exchange Hamiltonian used for **K-1**, for each of the trinuclear Mn_3 fragments, and a paramagnetic contribution associated with the Mn^{2+} ion linking the two sandwich fragments. The best least-squares fit values are $J_1 = -0.68\ cm^{-1}$, $J_2 = -1.14\ cm^{-1}$, and $g = 2.00$ ($R = 1.7 \times 10^{-4}$). The experimental low-temperature magnetization data are reproduced reliably on the basis of these parameters. The magnitude of the antiferromagentic exchange coupling is similar to that found in other Mn^{2+} sandwich-type polyoxotungstates.[7b,36]

Conclusions

We have prepared the three dimeric, sandwich-type tungstogermanates $[Cu_3(H_2O)(B\text{-}\beta\text{-}GeW_9O_{33}(OH))(B\text{-}\beta\text{-}GeW_8O_{30}(OH))]^{12-}$ (**1**), $[Co(H_2O)_2\{Co_3(B\text{-}\beta\text{-}GeW_9O_{33}(OH))(B\text{-}\beta\text{-}GeW_8O_{30}(OH))\}_2]^{22-}$ (**2**), and $[Mn(H_2O)_2\{Mn_3(H_2O)(B\text{-}\beta\text{-}GeW_9O_{33}(OH))(B\text{-}\beta\text{-}GeW_8O_{30}(OH))\}_2]^{22-}$ (**3**) in simple, one-pot reactions using an aqueous, buffered pH 4.8 medium. All three polyanions **1**−**3** have been fully characterized by single-crystal X-ray diffraction, FTIR, elemental analysis, and thermogravimetric analysis. The magnetic properties of **K-1**, **K-2**, and **K-3** have also been studied. We used Cu^{2+}, Co^{2+}, or Mn^{2+} to $[\gamma\text{-}GeW_{10}O_{36}]^{8-}$ ratios of 1.5:1 for the synthesis of **1**−**3**. Our results demonstrate that the reactivity of $[\gamma\text{-}GeW_{10}O_{36}]^{8-}$ with 3d metal ions in an aqueous acidic medium is similar to that of its silicon analogue $[\gamma\text{-}SiW_{10}O_{36}]^{8-}$. Both species can easily rearrange to different isomers of trilacunary "XW_9" and tetralacunary "XW_8" fragments which coordinate to the d-block metal ions, resulting in sandwich-type assemblies. We have shown that $[\gamma\text{-}GeW_{10}O_{36}]^{8-}$ is a highly flexible lacunary POM precursor which can adjust to the specific coordination requirements of the respective type of transition metal ion (e.g., Cu^{2+} vs Co^{2+}). We believe that **1**−**3** could also be interesting for homogeneous or heterogeneous oxidation catalysis applications. Currently, we are exploring the reactivity of $[\gamma\text{-}GeW_{10}O_{36}]^{8-}$ with other d- and f-block metal ions.

Acknowledgment. U.K. thanks the German Research Council (DFG-KO-2288/4-1), the Fonds der Chemischen Industrie, and Jacobs University for research support. A.H.I. appreciates a Ph.D. grant from the Ministry of Higher Education of the Arab Republic of Egypt. Figures 1−5 and Scheme 1 were generated by Diamond, version 3.1f (copyright Crystal Impact GbR).

Supporting Information Available: Thermograms of **K-1**, **K-2**, and **K-3** and X-ray crystallographic files in CIF format. This material is available free of charge via the Internet at http://pubs.acs.org.

(35) (a) Andres, H.; Clemente-Juan, J. M.; Aebersold, M.; Güdel, H. U.; Coronado, E.; Büttner, H.; Kearly, G.; Melero, J.; Burriel, R. *J. Am. Chem. Soc.* **1999**, *121*, 10028. (b) Clemente-Juan, J. M.; Coronado, E.; Gaita-Ariño, A.; Giménez-Saiz, C.; Chaboussant, G.; Güdel, H. U.; Burriel, R; Mutka, H. *Chem.—Eur. J.* **2002**, *8*, 5701. (c) Clemente-Juan, J. M.; Coronado, E.; Gaita-Ariño, A.; Giménez-Saiz, C.; Güdel, H. U.; Sieber, R.; Bircher, B.; Mutka, H. *Inorg. Chem.* **2005**, *44*, 3389.

(36) Gómez-García, C. J.; Coronado, E.; Gómez-Romero, P.; Casañ-Pastor, N. *Inorg. Chem.* **1992**, *32*, 3378.